

Gap bridging in joining of glass using ultra short laser pulses

Kristian Cvecek,^{1,2,*} Rainer Odató,³ Sarah Dehmel,³ Isamu Miyamoto,^{2,4} and Michael Schmidt^{1,2,3}

¹Chair of Photonic Technologies, Friedrich-Alexander-University of Erlangen-Nuremberg, Konrad-Zuse-Str. 3/5, 91052 Erlangen, Germany

²SAOT - Erlangen Graduate School in Advanced Optical Technologies, Friedrich-Alexander-University of Erlangen-Nuremberg, Paul-Gordan-Str. 6, 91052 Erlangen, Germany

³Bavarian Laser center (blz), Konrad-Zuse-St. 2-6, 91052 Erlangen, Germany

⁴Osaka University, 2-1 Yamada-Oka, Osaka 565-0871, Japan

*kristian.cvecek@lpt.uni-erlangen.de

Abstract: Glass welding by ultra-short laser pulses provides hermetic welding seams with high mechanical stability. The required distance between the samples must be extremely small (<100nm), otherwise cracks will form inside the seam reducing its stability. However, to achieve such small gaps the roughness of the samples must be small enough necessitating additional polishing. Additionally, Van-der-Waals forces grow substantial at such distances thereby effectively preventing sample movement and an easy and precise sample alignment. Here we present a method utilizing ultra-short laser pulses which exploits a volume expansion of irradiated glass enabling the joining of glass plates across gaps of up to 1µm.

©2015 Optical Society of America

OCIS codes: (350.3850) Materials processing; (320.7160) Ultrafast technology; (190.4400) Nonlinear optics, materials; (160.2750) Glass and other amorphous materials; (350.2660) Fusion.

References and links

1. H. Naumann and G. Schröder, *Bauelemente der Optik (Optical construction elements)* (Hanser Verlag, 1992) (in German).
2. H. Banse, *Laserstrahlöten – Technologie zum Aufbau optischer Systeme (Laser beam soldering - technology for the setup of optical systems)*, Ph.D-thesis, University Jena, Germany, (in German) (2005).
3. V. Greco, F. Marchesini, and G. Molesini, "Optical contact and van der Waals interactions: the role of the surface topography in determining the bonding strength of thick glass plates," *J. Opt. A, Pure Appl. Opt.* **3**(85), 85 (2001).
4. S. Hecht-Mijic, A. Harnisch, D. Huelsenberg, S. Schundau, J. Pfeifer, and T. Schroeter: "Thermisches Bonden von Bauteilen aus mikrostrukturiertem Glas," (Thermal bonding of elements made of micro-structured glass), *Mat.-wiss. u. Werkstofftech.* **34**, 645 (in German), (2003).
5. H. Maruo, I. Miyamoto, and Y. Arata, "CO₂ laser welding of ceramics," 1st International Laser Processing Conference (Laser Institute of America, 1981).
6. F. Grünwald, *Fertigungsverfahren in der Gerätetechnik (Manufacture processes in device engineering)* (Carl Hanser Verlag, 1985) (in German).
7. T. Tamaki, W. Watanabe, J. Nishii, and K. Itoh, "Welding of transparent materials using femtosecond laser pulses," *Jpn. J. Appl. Phys.* **44**(22), L687–L689 (2005).
8. T. Tamaki, W. Watanabe, and K. Itoh, "Laser micro-welding of transparent materials by a localized heat accumulation effect using a femtosecond fiber laser at 1558 nm," *Opt. Express* **14**(22), 10460–10468 (2006).
9. G. Haselhorst, Corporate Machinery and Production Technology, Process and Technology Development, Schott AG (manufacturer of D263 glass), Hattenbergstrasse 10, 55122 Mainz, Germany (personal communication, 2010).
10. Y. Okamoto, I. Miyamoto, K. Cvecek, A. Okada, K. Takahashi, and M. Schmidt, "Evaluation of Molten Zone in Micro-welding of Glass by Picosecond Pulsed Laser," *JLMN-Journal of Laser Micro/Nanoengineering.* **8**(1), 1–6 (2013).
11. K. Cvecek, I. Miyamoto, J. Strauss, M. Wolf, T. Frick, and M. Schmidt, "Sample preparation method for glass welding by ultrashort laser pulses yields higher seam strength," *Appl. Opt.* **50**(13), 1941–1944 (2011).
12. E. Sharon and J. Fineberg, "The dynamics of fast fracture," *Adv. Eng. Mater.* **1**(2), 119–122 (1999).

13. D. Hélié, S. Gouin, and R. Vallée, "Assembling an endcap to optical fibers by femtosecond laser welding and milling," *Opt. Mater. Express* **3**(10), 1742–1754 (2013).
14. Z. Tang, T. Shi, G. Liao, and S. Liu, "Modeling the formation of spontaneous wafer direct bonding under low temperature," *Microelectron. Eng.* **85**(8), 1754–1757 (2008).
15. I. Miyamoto, K. Cvecek, Y. Okamoto, and M. Schmidt, "Internal modification of glass by ultrashort laser pulse and its application to microwelding," *Appl. Phys., A Mater. Sci. Process.* **06**, 187–208 (2013), doi:10.1007/s00339-013-8115-3.
16. H. Scholze, *Glass. Nature, Structure and Properties* (Springer-Verlag, 1994).
17. Heraeus Group, Heraeus Quarzglas. (Online citation on July 1st 2014). http://heraeus-quarzglas.de/en/quarzglas/mechanicalproperties/Mechanical_properties.aspx
18. M. D. Perry, B. C. Stuart, P. S. Banks, M. D. Feit, V. Yanovsky, and A. M. Rubenchik, "Ultra-short-pulse laser machining of dielectric materials," *J. Appl. Phys.* **85**(9), 6803 (1999).
19. T. Yoshino, Y. Ozeki, M. Matsumoto, and K. Itoh, "In situ Micro-Raman Investigation of Spatio-Temporal Evolution of Heat in Ultrafast Laser Microprocessing of Glass," *Jpn. J. Appl. Phys.* **51**(10R), 102403 (2012).
20. *Physical Chemistry: Density, Standard Conditions for Temperature and Pressure, Vapor Pressure, Fick's Laws of Diffusion, Electrochemistry* (Books LLC, 2010).
21. K. Cvecek, S. Dehmel, I. Miyamoto, and M. Schmidt, "Ridge Formation on the Surface of Fused Silica processed by Ultra-Short Laser Pulses," In Proc. of LPM 2014, Vilnius, Paper Tu1-O-5, (2014).
22. K. Cvecek, I. Miyamoto, and M. Schmidt, "Gas bubble formation in fused silica generated by ultra-short laser pulses," *Opt. Express* **22**(13), 15877–15893 (2014).
23. K. M. Davis, K. Miura, N. Sugimoto, and K. Hirao, "Writing waveguides in glass with a femtosecond laser," *Opt. Lett.* **21**(21), 1729–1731 (1996).
24. D. M. Krol, "Femtosecond laser modification of glass," *J. Non-Cryst. Solids* **354**(2-9), 416–424 (2008).
25. Q.-Y. Tong and U. Gösele, *Semiconductor Wafer Bonding: Science and Technology* (John Wiley & Sons, 1999).
26. I. Alexeev, K. Cvecek, C. Schmidt, I. Miyamoto, T. Frick, and M. Schmidt, "Characterization of Shear Strength and Bonding Energy of Laser Produced Welding Seams in Glass," *JLMN-Journal of Laser Micro/Nanoengineering*, **7**(3), 279–283 (2012).
27. US Patent US20100084384
28. Y. Ozeki, T. Inoue, T. Tamaki, H. Yamaguchi, S. Onda, W. Watanabe, T. Sano, S. Nishiuchi, A. Hirose, and K. Itoh, "Direct Welding between Copper and Glass Substrates with Femtosecond Laser Pulses," *Appl. Phys. Express* **1**(8), 082601 (2008).
29. Y. Ozeki, H. Yamamoto, H. Yamaguchi, and K. Itoh, "Hermetic sealing of ceramic packages with glass by ultrafast laser welding technique," In: Proc. LAMP 2009, Paper MoOL 1-7, 09-115, Kobe, Japan, (2009).

1. Introduction

Glass is a versatile material and is used as such in optics, electronics or biomedicine. However, the actual applications most often require an assembly and subsequent joining of several glass parts. Although established methods for glass joining exist, they have nonetheless limitations that make them highly application-specific. In general, joining methods that use additional material such as in mechanical mounting [1], gluing [2] or soldering suffer often from a mismatch of thermal expansion coefficients between glass and mount material, glue or solder. This limits e.g. the temperature range in which such composites can be used. Conversely, conventional joining technologies without additives are e.g. optical contacting [3], thermal diffusion bonding [4] or CO₂-laser welding [5]. Here again the methods are not suited for all purposes: optical contacting is susceptible to impact loads [6], thermal diffusion bonding requires long processing times and CO₂-laser welding requires a subsequent post-heating.

In contrast to this, a promising, alternative approach offering a much higher versatility is fusion welding of glass using ultra short laser pulses (USP lasers).

This process has been shown first by [7,8]. The achieved seam strength was approximately 10 MPa. Although the joining was successful the achieved strength was far from strengths exhibited by bulk material which lies in the range of 100-200 MPa [9,10]. One of the reasons for this relatively low bonding strength bonding lies probably in the fact that the samples were pressed against each other during the welding in order to minimize the gap. This in turn might have led to internal tensions after welding when the glass samples relaxed to their initial state, leading to considerable mechanical stress on the welding seams. However, the observed low strength of the welding seams might have another origin in a possible residual gap between the samples, even though the plates were pressed together.

As we were able to show in [11] at gaps larger than 0.4 μm cracks can occur inside the welding seam. Though the glass plates are connected by glass material to each other the cracks will strongly reduce the strength of the seam since an applied load can cause nearly singular stress fields at the tips of the crack [12], thus enabling further crack growth. In order to reduce the gap we proposed closing the gap between the glass plates by providing optical contact between the samples, so that no external forces had to be applied while achieving a gap width smaller than 100 nm. As a result we achieved crack-free welding seams that exhibit strengths and bonding energies that are on par with those of bulk glass material. Furthermore, the beneficial influence of preparing optical contact between the glass samples prior to welding has been shown also by [13].

Optical contact is provided when two conjugate (glass) surfaces are so close to each other that they are bound by Van-der-Waals forces. The range of these forces is limited to a few hundred nanometers, because the attracting potential for two plane surfaces reduces as $1/d^2$ with distance d [3]. The optically contacted area lacks reflections from the joining surfaces, since the gap is so small that that evanescent waves generated by an impinging light wave at the surface of the first glass plate excite, almost without attenuation, a propagating wave inside the other plate. Typical values necessary for optical contact of two plane plates are <0.5 nm surface roughness, <5 μm total thickness variation, and <30 μm flatness [14]. Although it is possible to achieve optical contact with higher values, the optical contact may not cover the whole area of the plates.

The underlying mechanism that leads to cracks in case of a gap or to crack-free welding seams in the presence of optical contact has been described in detail in [15] but is outlined briefly in the following because it is crucial for understanding the effectiveness of our gap bridging method:

For sufficiently large gaps the glass melt from the welding seam can escape into the gap. Since the melt has low viscosity any internal compressive stresses of the melt (due to high temperature and plasma pressure) will relax almost completely as the melt escapes into the gap. Therefore, in the presence of a gap the melt will be free of tension or pressure as long as it is still fluid. During the cool-down the glass starts to solidify which applies to the glass inside the welding seam as well as to the melt that escaped into the gap. The solidification itself can be assumed to be strain-free due to the previous relaxation of the melt. However, since the solidification temperature is quite high for glass [16] further cool down to room temperature will result in thermal shrinkage of the glass. Consequently, tensile stresses are formed during the shrinkage process of solidified glass. But glass is by more than a factor of 20 more sensitive to tensile than to compressive stresses [17], so this leads very easily to cracks.

In contrast, a molten zone, enclosed by bulk material, will expand during irradiation and melting and will strain against the adjacent material. However, if the melt zone is not too large, the adjacent bulk material will be able to withstand the stresses. In the following cool down the glass will shrink back – especially if disregarding any permanent residual material changes – to its previous volume. As a result the molten zone induces no cracks during solidification and shrinkage while cooling down. From this viewpoint optical contact encloses the hot melt by Van-der-Waals forces at the welding interface and, simultaneously, prevents leakage of the molten glass into the gap by having virtually no gap. Therefore, welding optically contacted glass samples provides crack-free welding seams.

However, as mentioned above, the glass plates have to fulfill high requirements concerning the surface quality in order to make optical contact achievable. The necessary polishing to achieve this quality is very time consuming and thus very costly to be of use in industrial applications. Besides this, it is not only the polishing costs that are detrimental to a wide-spread use of the USP laser glass welding technology in industry. Since one of the main advantages of USP laser glass welding is the very small welding seam the glass welding process excels when very small or heat sensitive glass components such as MEMS have to be

joined. But in many cases the components to be welded have to be aligned, often with a tolerance of few micrometers. Unfortunately, providing alignment after the samples have been optically contacted is very hard to do due to the Van-der-Waals bonds. Likewise, precise sample alignment before optical contacting has also a drawback, since, depending on the exact contacting process, application of high forces can become necessary. In this case, in order to provide such high forces with a positioning precision on the micrometer scale expensive equipment must be acquired.

The above mentioned difficulties in obtaining optical contact was the reason we strove to improve the “conventional“ USP laser glass welding process. This novel process does not require optical contacting and enables to bridge the residual gap. This helps to relax the requirements on the glass samples' surface while it allows fine-positioning of the samples before welding due to the residual gap. In the following we outline the underlying physical mechanisms, describe the experiment, show and discuss the results and will comment on possible future applications that can be realized by this process.

2. Method

The method is similar to glass welding by ultra-short laser pulses described in [7,8,10,11,13,15], where laser pulses at a wavelength transparent to glass are tightly focused near the joint surface of two glass parts. Due to the tight focusing and short laser pulse duration, the light intensity inside the focal volume reaches values high enough to achieve multi-photon absorption [18]. (For pulse durations well below 100 fs also tunnel and field ionization may occur instead.) The freed electrons can act as seed electrons for avalanche ionization (within the same laser pulse). Once started, the avalanche ionization can carry on even if the pulse intensity drops below the value necessary for multiphoton ionization. During irradiation the electron plasma builds up very quickly and reaches very high temperatures. Subsequently, the plasma as well as the adjacent material are heated by electron-phonon coupling. Numerical simulations [15] show for a steady-state case (at sufficiently high pulse repetition rates) that the plasma may easily reach average temperatures between 3000 and 4000 K. But high temperatures in the wake of the focal spot were also measured experimentally by Raman spectroscopy [19]. For better understanding a typical temperature distribution (in this case D263 borosilicate glass) is shown in Fig. 1 (compare [15]).

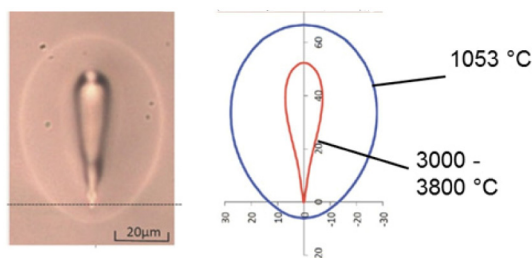


Fig. 1. Cross section of a typical molten zone in D263 with the corresponding calculated temperature distribution [15].

Figure 1 shows that very high temperatures are reached inside the processed region. This in turn leads to substantial heating close to the processed region by heat conduction. However, this means that due to the strongly temperature-dependent viscosity of glass (compare Fig. 2) the glass is in the vicinity of the molten region moldable. If this region is placed near the glass surface, the surface becomes also moldable, since the surface tension is also lowered at the high temperatures [20]. However, as long as the temperature at the surface is not too high, the surface tension will prevent an expulsion of the liquid glass melt from the molten zone below the surface and will thus not lead to a jagged surface of the bulge. Instead the surface tension will provide smoothened bulges.

Since the achieved temperatures inside the molten zone and plasma are quite high, thermal expansion of the molten glass as well as the plasma will exhibit a pressure that will lead to a reversible bulging of the surface – as long as the surface temperature is high enough for the glass to be moldable. The schematic of the bulging mechanism is shown in Fig. 3.

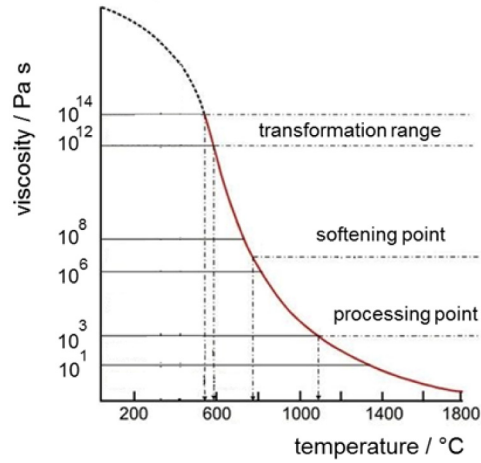


Fig. 2. Schematic diagram of temperature dependent viscosity of glass (compare [16]).

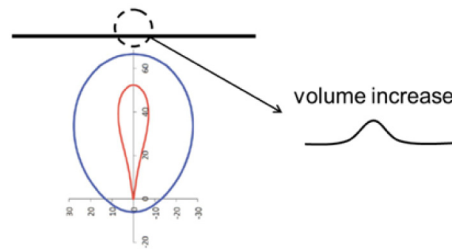


Fig. 3. Schematic diagram showing the expected surface alteration of a closely positioned molten area in case of volume increase or decrease.

If the height of the bulging is high enough to bridge the gap to the second joining partner and the glass is still moldable the soft surface of the bulging will adapt to the surface shape of the joining partner. Due to its softness it is to be expected that if the surface gets close enough to the other glass surface Van-der-Waals forces will start to act between the surfaces. Depending on several parameters of the bulge getting into contact with the other surface such as achieved proximity, duration of the contact and temperature there might be even diffusion of silica chains into the adjacent joining partners resulting in a localized diffusion bonding, instead of only achieving an optical contact with a relatively low bonding strength.

Of course due to the constant feed speed the focal spot will move on and leave the currently heated soft surface that has bonded in a kind of localized optical contact or diffusion bond to the other joining partner. In consequence, the melt zone below the surface of the bulge will start to cool down and thus to shrink. However, in contrast to direct gap welding, in this case the melt does not have the opportunity to relax its pressure, since the surface tension of the bulge prevents a rupture of the surface. Therefore, the situation is still similar to generating melt runs in bulk material and no cracks will be generated. Due to the local bond between the bulge and the other joining partner the shrinkage will induce a closing of the original gap between the welding partners as the shrinking bulge will exhibit a pulling force on the joining partner via the bond.

Interestingly, as shown first in [21], a residual surface bulging can additionally be observed at room temperature. In [21] only Fused Silica was investigated. The observed irreversible bulging was on the order of 50 nm which is rather small and occurs very likely due to the pressure of oxygen gas bubbles generated in the heat accumulation regime [22]. The pressure of the generated gas bubbles overcomes the volume reduction of the densification effects of USP laser induced refractive index increase [23,24]. However, as is shown in the experimental results (section 4, Fig. 7) the irreversible volume increase occurs also in several other glass types such as Borosilicate and Soda Lime glass where the gas bubble formation is not as prominent as in fused silica. Obviously, the laser induced material changes lead to a distinct irreversible increase of the volume. Moreover, the observed volume increase is even bigger in Soda Lime and Borosilicate glasses than in Fused Silica, even though the gas bubble generation is much less effective in these glass types.

The irreversible volume increase is actually beneficial for the joining. This is especially true if the glass samples do not have a very high surface quality so that optical contact cannot be established. In such a case the surface deviations are typically too large to establish Van-der-Waals bonds over the whole surface since the Van-der-Waals forces would then have to overcome the bending and compressional energy necessary to make the surfaces lie flat against each other. Consequently, though a purely reversible volume expansion would be able to establish in this case some Van-der-Waals bonds when the material is still hot, the bonding would not provide enough energy to keep the bond closed during the shrinkage process. In contrast, an irreversible bulge will act as a spacer inside the gap. In turn the strain on the bond will be lower as the glass plates do not have to bend too far from their respective unstressed condition before joining. Correspondingly, the seam strength will be improved while the requirements on sample surface quality can be kept lower.

3. Experiment

In this section the glass irradiation and welding processes are described as well as the measurement procedures. The schematic of the experimental setup is depicted in Fig. 4. The laser used has a FWHM-pulse duration of 10 ps at 1064 nm and its pulse repetition rate of the laser was kept for all experiments at 1 MHz and the average laser power at 2 W. The laser beam is focused by an IR microscope objective with a numerical aperture of 0.55 into the sample which is mounted on an x-y-translation stage. The samples were aligned horizontally first by measuring the distance from the microscope objective to the upper surface of the sample for several x-y-positions than by tilting the sample by an according tilt angle calculated from the height measurements. The glass samples were prepared depending on whether they were intended for the observation of the surface bulge or for the observation of joining by gap bridging.

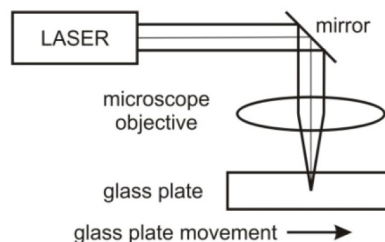


Fig. 4. Schematics of the setup used for glass irradiation experiments.

For surface bulging experiments only single glass plates were used and the laser processing started at a displacement of $-230\ \mu\text{m}$ below the surface. Please note that the given displacement values are the values of the mechanical displacement of the z-stage. Due to the refractive index of the glass (which is roughly 1.5 for all analyzed glass types) the true focal

position is by the same factor deeper inside than the mechanical value. Then the sample was laterally displaced to irradiate new unmodified glass material while the focal position was increased by 2 μm towards the surface while keeping all other parameters constant. If the displacement of the focal spot to the surface became too small resulting in obvious surface damage, the procedure was stopped and repeated with different feed speed or different glass type. The surface bulging was analyzed by a confocal laser scanning microscope with a 10 nm height resolution. In order to achieve a sufficiently high signal to noise ratio for the measurement of the deformation we found it necessary to increase the reflectivity of the glass surface by sputtering it with a thin layer of gold.

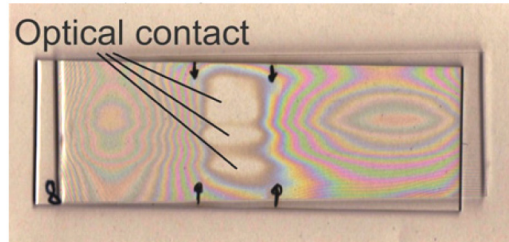


Fig. 5. Photograph of sample prepared for joining experiments. The extents of the optical contact area are marked by arrows. The interference fringes are visible on both sides of the optical contact as multicolored stripes.

For the welding experiments the samples were brought in close contact by establishing locally an optical contact as shown in Fig. 5. The area where optical contact was present has been marked so that welding seams could be placed outside of the optical contact area where interference fringes indicate a small but definite gap. This approach has the benefits that the gap width can be approximately determined by analyzing the number and sequences of the color fringes while no external forces are necessary to keep the samples close to each other. The prepared gap heights for all samples were between 250 nm and 1 μm . After performing the tilt correction the lower surface of the upper glass plate was found by the confocal surface measurement procedure. The detected position of the rear surface of the upper plate has been used as the reference height from which the focal spot is displaced. The displacement length was chosen accordingly to the glass type within an interval of $\pm 4\mu\text{m}$ (in steps of 2 μm) around the optimum focal spot displacement determined in the bulging experiments. For each z-position a group of 20 melt runs with a lateral spacing of 300 μm was performed.

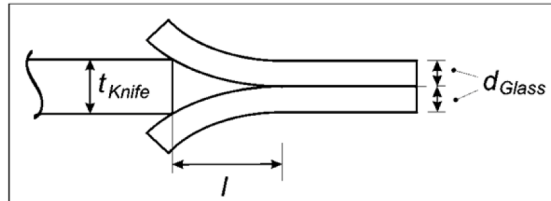


Fig. 6. Schematics of the crack opening test.

After processing the samples were optically analyzed whether joining has been achieved or not. If the joining was successful the joining seams were characterized by the crack opening test (COT) [25]. The COT method offers a possibility to characterize the joint in terms of bonding energy. However, as it is applied in wafer testing where the joining area exhibits roughly the same bonding energy over its entire extents it has to be slightly modified in order to characterize the quality of the welding seam only.

In this procedure, a knife edge with thickness t_{Knife} is inserted between the glass plates which are bonded either by Van-der-Waals forces (optical contact) or by covalent bonds

(welding seam). The knife opens a crack between the plates (see Fig. 6). The length l of this crack is determined by the minimum of the total energy necessary for crack opening. This energy consists of the work needed to separate the glass surfaces and the potential energy necessary to bend the plates. In the case of glass plates with equal height d_{Glass} and elasticity module E the bonding energy γ is given by Eq. (1) (for further reading see [25]):

$$\gamma = \frac{3 \cdot t_{Knife}^2 \cdot d_{Glass}^3 \cdot E}{32 \cdot l^4} \quad (1)$$

4. Experimental results

4.1 Observation of ridge formation

Examples for surface bulging induced by laser irradiation (as described in section 2 Fig. 3) are given in Fig. 7 for all analyzed glass types which shows the surface height by color coded diagrams. (Please notice the different scaling ranges). While the bulging behavior varies in terms of size and smoothness for the different glass types it is clear that in each image there are two melt runs present. The processing conditions for the samples in Fig. 7 are given in Table 1 (the smaller displacement corresponds to the highest ridge).

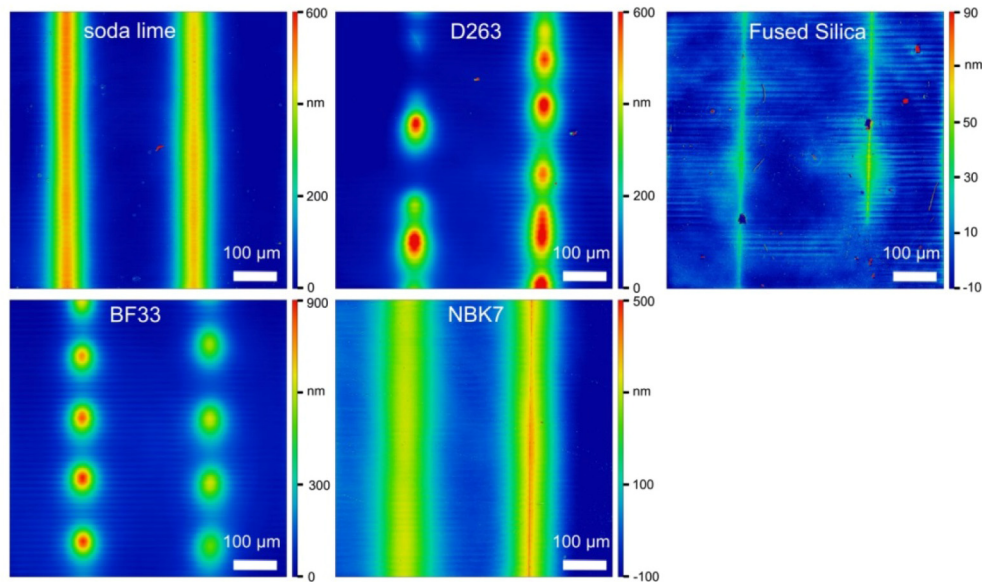


Fig. 7. Confocal microscope height measurements of selected samples of different glass types. Please notice the different scaling ranges.

Table 1. Processing Parameters Used for Samples Shown in Fig. 7

Glass type	Soda Lime	NBK7	BF33	D263	Fused Silica
Feed speed in mm/s	15	2	5	2	1
Focal displacement from surface in μm	124;126	112;114	94;96	86;88	44;46

The overview of the achievable bulging heights plotted against the displacement of the focal spot below the surface for all investigated glass types is given in Fig. 8. Since the length of the melt runs is much larger than the field of view of the confocal microscope, only heights within the same field of view as shown in measurements in Fig. 7 have been evaluated. Thus, the data points show rather a tendency than an all-encompassing description of the bulging

behavior. The bulging height of all processed samples was measured along the maximum of each ridge for every focal displacement below the glass surface. The reader may note that the number of data points in Fig. 8 is different for the glass types and feed speeds. The reason for this is that for some parameters either no bulging was observed or that the glass surface was severely cracked (both effects are very pronounced in fused silica). Since several glass types show also a kind of localized bulging probably due to underlying dynamic processes (compare

Figure 7 BF33 and D263) we choose to evaluate the average height. Consequently, the maximum achievable height can be larger than the one shown by the data points in Fig. 8.

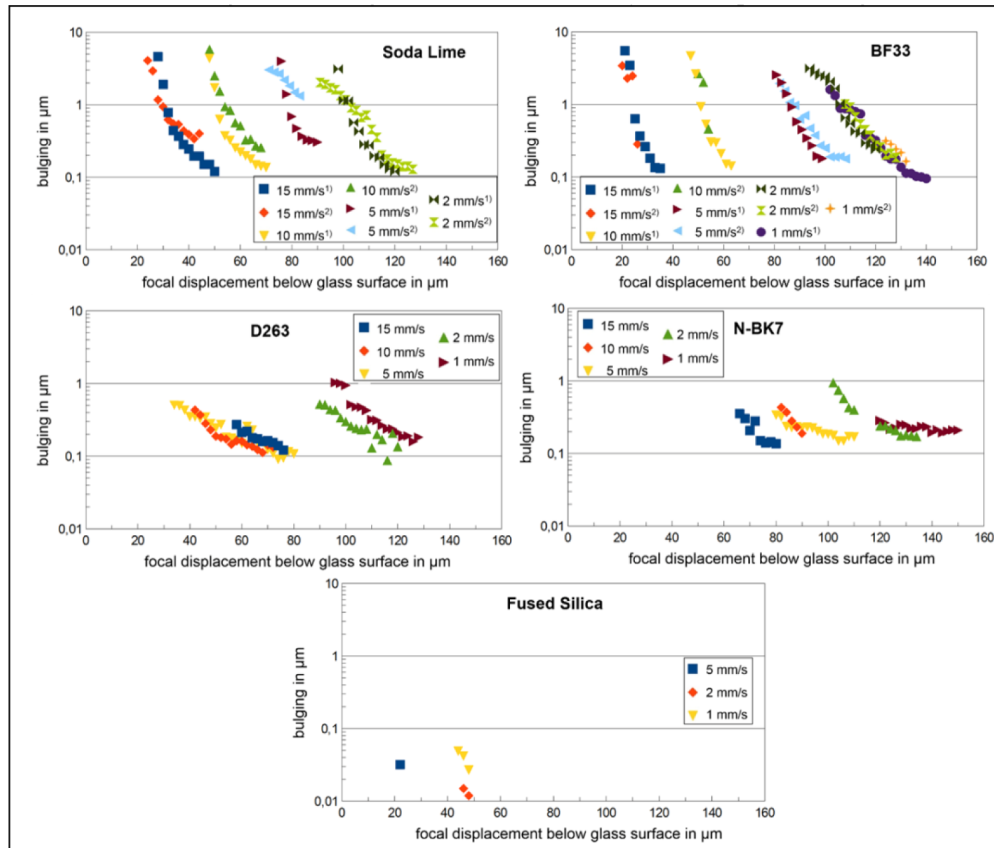


Fig. 8. Measured average bulging height depending on the focal displacement below the glass surface for different feed speeds and glass types. The superscript cases 1) and 2) (Soda Lime and BF33) depict two different experiments conducted under otherwise same conditions.

As can be seen in Fig. 8 the range of the focal displacements from the surface where a ridge formation can be observed can be as wide as 30 μm for a given feed speed. Depending on the glass type the maximum bulging height can achieve values up to several microns. However, especially if a gap of more than 1 μm has to be bridged then the range of possible focal displacements is severely limited due to the steep slope of the dependence of bulging height on focal displacements. Consequently a focal positioning with an accuracy of better than 1 μm is necessary to achieve consistent results.

4.2 Glass joining across a gap

Figure 9 shows the results of the welding across the gap as explained in section 3, page 7. Each glass sample is shown after welding. As can be seen, except for N-BK7 glass, for each

glass type a successful gap bridging has been achieved. It has to be noted that the surface quality of the glass samples was different. While for Fused Silica, D263, N-BK7 and BF33 the surface quality was high enough to easily obtain optical contact, the surface quality of Soda Lime glass was just barely high enough to obtain local optical contact. In the first case we had to be careful to provide only local optical contact, while we had to struggle to obtain it in the second case.

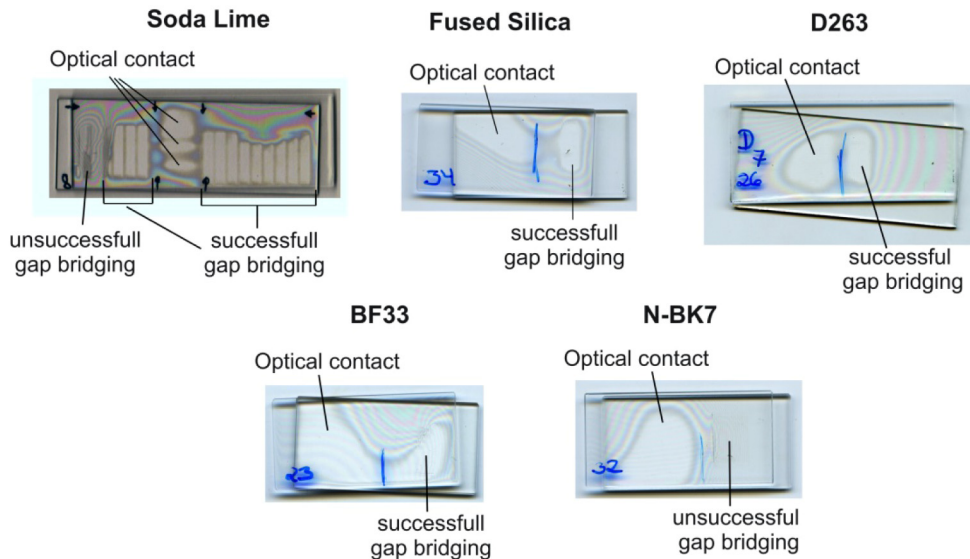


Fig. 9. Glass samples prepared with optical contact and marked optical contact boundary processed by USP laser for gap bridging.

The bridging observed in Fig. 9 can be explained with Fig. 8. While the Soda Lime glass used in the experiment has had a low surface quality it provides very high irreversible bulging by which the gap can be bridged despite the “wavy” surface. BF33 and D263 have somewhat similar thermodynamic and bulging properties of Soda Lime glass and in conjunction with the outstanding surface quality of the samples gap bridging was provided in all analyzed samples. Figure 8 shows that Fused Silica has a very small irreversible bulging. But as described in section 3 the reversible thermal expansion is nonetheless present and in combination with the very high surface quality the gap can still be obviously bridged. Only the unsuccessful bridging in N-BK7 samples cannot be readily explained since the samples had also outstanding surface quality and, as Fig. 8 shows, a high irreversible bulging. A possibility for the negative result in joining N-BK7 could still be caused by unnoticed misalignment (error) of the welding system during the joining experiments. Thus the applicability of the described gap bridging method will have to be investigated in more detail for N-BK7 glass in future experiments.

Of course, a simple optical analysis is not sufficient to prove that a gap bridged by USP laser processing is a joint capable of transferring bonding forces. Therefore we measured the bonding energy of the joints by the COT-method as described in section 3, page 7. The results for all glass types (except N-BK7) are shown in Fig. 10. For comparison reasons the bonding energy of an optical contact was also measured by the COT method and amounts to 0.1 ± 0.03 J/m² which lies well within the limits for optical contact bonding energies between 0.05 and 0.23 J/m² known for prebonding processes [25]. It can be seen that the bonding energy, including the error bars, is higher than the bonding energy of the optical contact. For D263, Fused Silica and BF33 the average value lies around 1.5 and 2 J/m² which corresponds well to the bonding energy of 2 J/m² of a glass pair that was diffusion bonded at 800 °C [25]. The

bonding energy for Soda Lime was somewhat lower but this could probably be attributed to the low surface quality resulting in a pre-stress and thus effective decrease of the measurable bonding energy. However, all results imply that the described gap bridging process provides not only Van-der-Waals forces between the joining partners but also true chemical bonds.

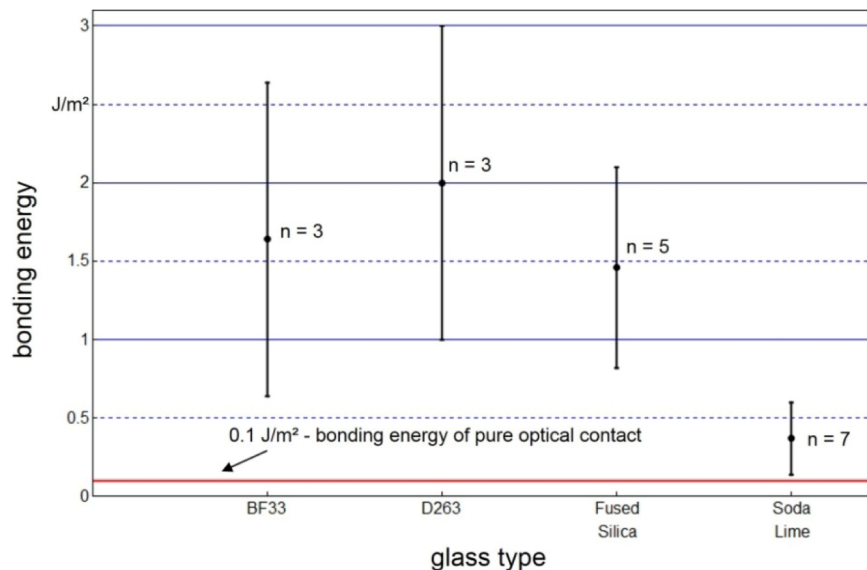


Fig. 10. Measurements of bonding energy for the described gap bridging process.

5. Discussion

The development of true chemical bonds during the glass joining process described here is also supported by the structure seen in microscope images of peeled-off welding seams as depicted in Fig. 11. Clearly, there is additional glass material attached to the typical structure of zone molten (compare Fig. 1). Moreover, it is possible to bridge the gap from each glass plate, either by creating the bulging at the lower surface of the top glass plate (see Fig. 11 (a)) or, as done in the experiments described in sections 2 - 4, by creating the bulging at the upper surface of the lower glass plate. Of course, the generation of the bulging at the upper facet of the lower glass plate side is by far more consistent due to the smooth upper area of the typically tear drop shaped molten zone than it is for the tip the lower facet of the upper glass plate.

A similar glass joining process has been described by Bovatsek et. al. in [27] where a twofold irradiation of the glass is necessary to achieve joining. The first irradiation run provides the bulging without joining. Then a second irradiation run is carried out on the same area as before, displaced only along the optical axis to provide a better focal position, is used for the joining. However, an analysis of the underlying processes, the achievable bridging heights, the usable glass types as well as the achievable mechanical bonding energy or joining strength is not given in [27]. We believe that the same process of irreversible volume expansion as described in this work is responsible. In contrast to [27] the process we have described here works with a single irradiation of the joining area and is therefore faster than the process in [27]. Moreover, it is our opinion that a second irradiation at the joining seam actually decreases the bonding strength, because the twofold irradiation introduces a larger irreversible volume expansion and hence the induced stresses increase even further.

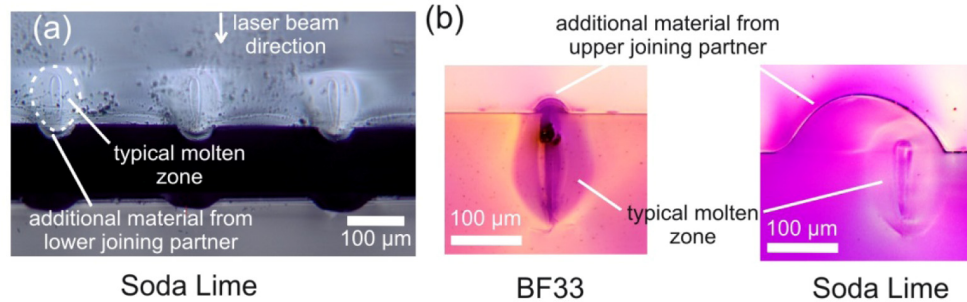


Fig. 11. Cross sections of peeled off joining seams with focal spot within the upper glass plate (a) and lower glass plate (b).

When compared with bonding energies provided by USP glass welding of prebonded glass samples (without a gap) [26], the results here show that a prebonding is not necessarily needed in order to achieve high bonding energies of the joint. A possible reason for this might be that the first irradiation provides a joint between the glass plates that leads to a reduction of the gap. Subsequent irradiation runs next to the first irradiation have to bridge an ever smaller growing gap (in case of high surface quality). Thus it seems to be that high surface quality is ideal to achieve such high bonding energies as shown by the difference between Soda Lime glass and the other investigated glass types in Fig. 10. This means especially for glass types such as Fused Silica or BF33 which have a low irreversible volume expansion (see Fig. 8) a good surface quality has to be provided. Otherwise, the forces necessary to achieve the bending of the glass parts for joining might be too high.

Of course there are several open issues that prevent so far a direct industrial implementation of the here described joining process. These issues are pointed out in the following. First of all the experiments conducted here were intended to be proof of concept. That is why as of now we cannot give reliable values as to the bridgeable height. As can be determined from Fig. 5 and 9 the bridging occurs at heights of 1-4 Newton stripes in reflection. These stripes correspond at white light irradiation to gap heights between approx. 130 nm – 1 μm. Subsequent experiments are planned to answer this question in more detail.

However, independently of the actual gap width at which joining can be realized, it is still clear that the bridgeable distance will not be much larger than probably 1 μm. While in such case the samples can be precisely positioned to each other it is yet unclear how to mount the samples without optically contacting them as done in this work. A possible answer to this is probably given in [7] where the samples were pressed onto each other by a large pressure. As pointed out in the introduction due to mechanical tensions this could have reduced the mechanical strength of the welding seam. Of course, it could have been that, unwittingly, a similar process has been applied as described here or in [27], especially as the authors state that the focal spot was focused directly onto the joining surface, which also results in a joint (compare Fig. 11). Nonetheless, even if a gap of up to 1 μm can be bridged, the waviness of the glass plate has to be still quite small.

Finally, any mounting method striving to achieve such small gaps will have to be characterized by measuring the gap width. While the measurement is quite easy while an optical contact is present by counting the Newton stripes (assuming the gap grows monotonically bigger), things become more difficult, if no optical contact is established. Without optical contact present there is no reference height of zero gap from which to number the Newton stripes for gap width calculation. Other ways to evaluate the gap are similarly problematic. For confocal microscopy using near UV light the adjacent surfaces have to be at least approximately 600 nm apart, otherwise the signals from both surfaces will overlap. Similarly, conventional state of the art optical coherence tomographs using ultra-wide band light sources achieve similar axial resolutions around 1 μm. The only apparent workaround is

to measure the thickness of the glass plates separately before assembling them in the mount. After mounting the samples the gap can be estimated by measuring the total width of the mounted glass plate by subtracting the separate (beforehand measured) glass plate thicknesses.

6. Conclusion and outlook

In this work a glass joining process based on ultrafast laser pulse irradiation is described that does not require the preparation of optical contact as described in [11,26]. Instead, reversible thermal expansion in combination with irreversible volume increase of processed glass is exploited in order to bridge a small gap between the joining partners. This joining procedure establishes Van-der-Waal forces as well as chemical bonds between the joining partners, thus exceeding the pure Van-der-Waals bonding energy of a pure optical contact. The achieved bonding energies ranged between 0.4 and 1.6 J/m². The height of the gap to be bridged ranged from 130 nm up to 1 μm.

The benefits of this glass joining process are that glass plates can be joined without the need to establish optical contact. This is highly advantageous since without prebonding the samples can be precisely aligned before joining, the prebonding step can be skipped and glass samples can be used for joining that have a lower surface quality than necessary for optical contacting, thus reducing the costs.

Of course, this is only possible insofar as long as the bending strain and the irreversible bulging can cope with each other. As pointed out in section 5 this might be critical for Fused Silica. However, as presented in [22] in Fused Silica oxygen bubbles are generated that can be dragged along with the focus of the laser. This effectively means that the described glass joining and gap bridging process can be conducted in such a way that gas bubbles are first generated and collected inside the melt run for bridging the gap between the glass plates.

Nonetheless, the most interesting implication of the described joining process is the fact that the bulging hot glass melt establishes Van-der-Waals bonds to the other joining partner across the gap. The other joining partner does not have to be necessarily glass. It should be sufficient, if it is a material that is wettable by molten glass and has a melting point that is either higher or lies in a similar range as achieved temperature of the surface which may be lower than melting point of the glass itself. If the material is wettable by glass, Van-der-Waals forces will be provided effectively creating at least a prebonding by optical contact. Molecular diffusion or creation of chemical bonds is in such case not really necessary. This way, the described method can open possibilities to join chemically dissimilar materials with glass. In this regard there exist several publications that describe the joining of dissimilar materials with glass such as silicon-glass [15], metal-glass [28] or ceramics-glass [29] and it is very likely that the herein described method should work also for these material combination or that similar processes as described here can be found also in those processes. However, the here described method should be also theoretically applicable for joining of mechanically hard materials such as diamond or tungsten carbide or materials with slightly lower thermal damage threshold than glass such as joining of Fused Silica with UV-transmissive salts or nonlinear optical crystals.

Acknowledgments

This work was supported by the Bayerisches Laserzentrum GmbH Erlangen (blz), the Erlangen Graduate School in Advanced Optical Technologies, Friedrich-Alexander University Erlangen-Nürnberg (SAOT) as well as the Deutsche Forschungsgemeinschaft and Friedrich-Alexander University Erlangen-Nürnberg (FAU) within the funding programme Open Access Publishing.